Grating couplers for surface plasmons excited on thin metal films in the Kretschmann-Raether configuration

U. Schröter and D. Heitmann
Institut für Angewandte Physik und Zentrum für Mikrostrukturforschung, Jungiusstraße 11, 20355 Hamburg, Germany
(Received 23 February 1999)

We investigate the optical properties of periodically modulated thin metal films in the Kretschmann-Raether configuration. We find that excitation of surface plasmons via the grating coupler effect at the metal surface not facing the incoming light is not possible in the case of a conformal modulation of the two metal surfaces, but only if the thickness of the metal film is varied over the grating period. In this case there is strong interaction between the surface plasmons on both surfaces and photonic band gaps open up in the dispersion. Whereas in reflection spectra the surface plasmons are seen as minima, they can appear as maxima, minima, or Fano-type resonances in transmission spectra. We show how thin film grating couplers can be tailored to achieve a field strength enhancement at a particular interface or pronounced photonic band gaps. [S0163-1829(99)00931-5]

I. INTRODUCTION

Surface plasmons[1] are electromagnetic excitations that propagate along the interface between a metal and a dielectric. The fields are highest at the interface itself and decay exponentially into both media. But this field enhancement is not the only reason why surface plasmons may become interesting for optical applications.[2–5] A periodical modulation or grating structure of the surface opens further possibilities. Barnes and co-workers[6,7] presented textured surfaces that exhibit photonic band gaps analogous to photonic solids. Recently, they examined a layer structure with a microcavity. One mirror of that microcavity had a periodically modulated surface.[8] This results in photonic band gaps for coupled surface plasmon polariton modes of the cavity. Whereas the approximate positions in frequency and wave vector of the surface plasmons and the photonic band gaps can be easily anticipated from the periodicity of the grating, it is more difficult to predict the strengths of the excitations. Sometimes astonishing behavior is observed. Ebbesen and co-workers[9,10] investigated the optical transmission through arrays of small holes in relatively thick metal films on quartz substrates and found extraordinarily high transmission peaks in their spectra. These are due to surface plasmons on either side of the metal film.[9–11] Surprisingly, the transmission strengths are the same, regardless of whether the illumination is from the air or from the substrate side.

A surface plasmon on a single flat interface between a metal and a dielectric cannot be excited simply by radiating light onto that surface, because the wave vector of the plasmon parallel to the surface exceeds the wave vector of light of the same frequency in the dielectric [Fig. 1(a)]. Periodical modulation of the surface with a period a [Fig. 1(b)] introduces a grating coupler which can add a multiple of $2\pi/a$ to the wave vector parallel to the surface. As part of the dispersion branches thus come to lie inside the light cone [Fig. 1(c)], for certain angles of incidence depending on the frequency light can now couple to surface plasmons. A second way of enlarging the wave vector is an attenuated total reflection setup [Fig. 1(d)]. In this case, one uses a thin layer of metal and the light is incident from a second dielectric $D2$ that has a larger index of refraction than the first dielectric $D1$. Then the wave vector for light of a certain frequency is lager in $D2$ than in $D1$. If the metal film is thin enough, the light can ''tunnel'' through it and excite a surface plasmon at the interface between the metal and $D1$. But as the dispersion curve of the surface plasmon lies entirely to the right of the light line in $D1$, for excitation of surface plasmons angles of incidence greater than the total reflection angle between the two dielectrics are needed.

In this paper we investigate what happens if we modulate one or both interfaces in Fig. 1(d). The question is whether a periodic texture can help to excite surface plasmons at small angles of incidence not only at the interface between the metal and $D2$, but also at the interface between the metal and $D1$. The Kretschmann-Raether setup allows us to spatially separate the evanescent plasmon field from the incident and

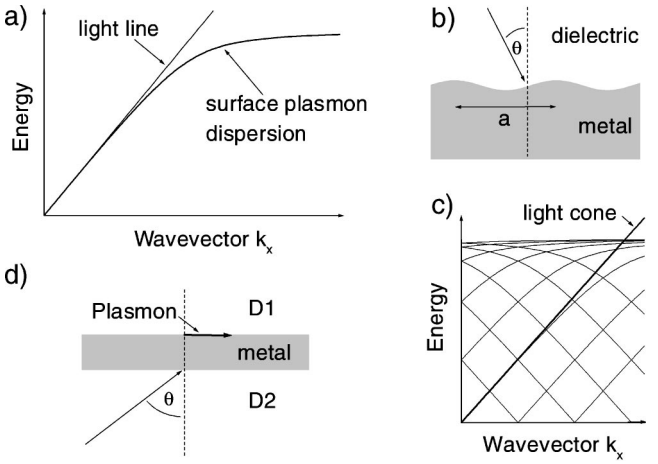

FIG. 1. (a) Dispersion for the surface plasmon on a planar metal-dielectric interface. (b) Periodically modulated metal surface and (c) surface plasmon dispersion for the grating. Possible band gaps at the crossing points of the branches have been neglected in this scheme. (d) Attenuated total reflection setup with a thin metal film between two dielectrics $D1$ and $D2$. $D2$ has a higher index of refraction than $D1$.

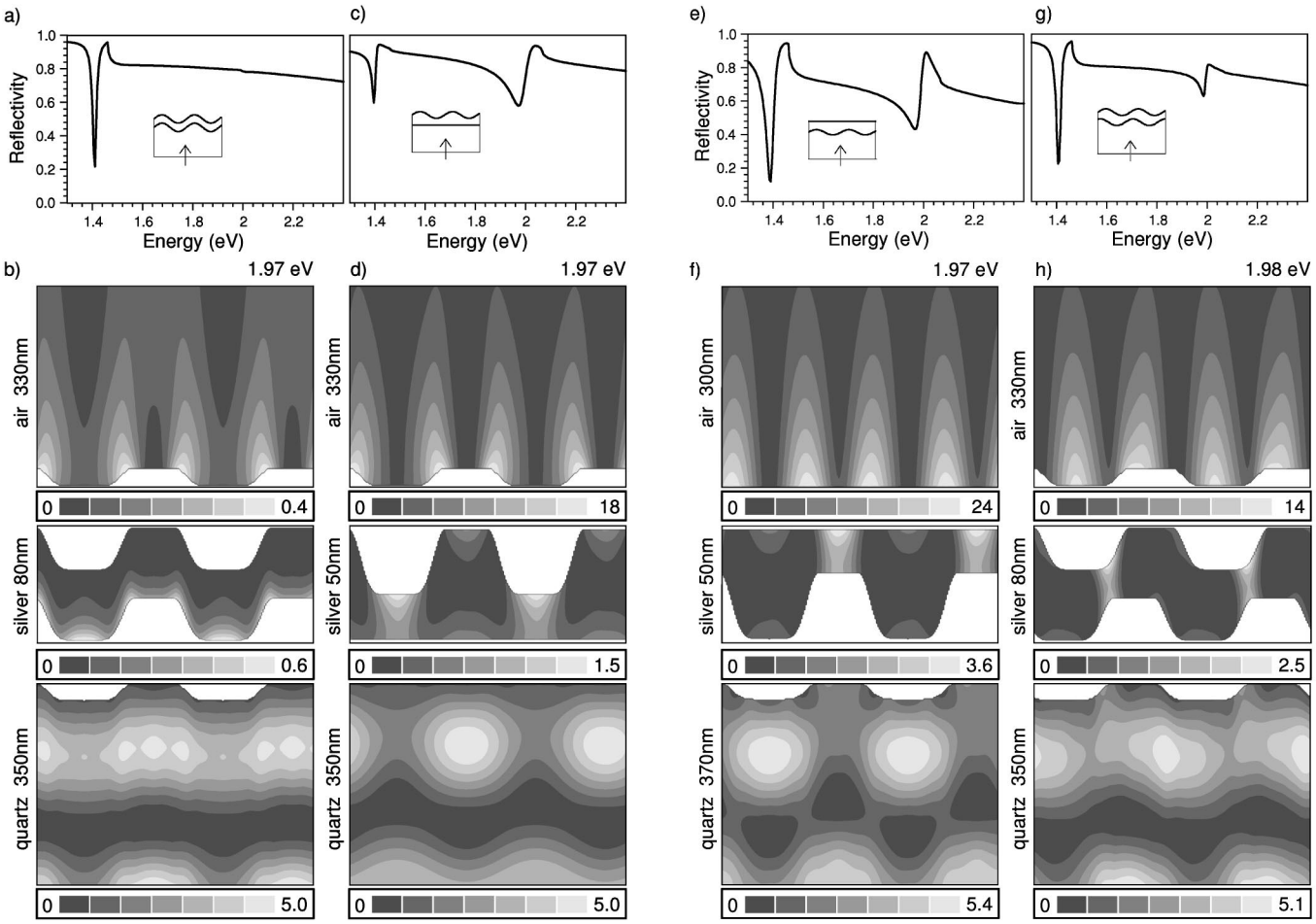

FIG. 2. Calculated reflection spectra for normal incidence from the substrate side for 600-nm grating and near-field distributions ($|\vec{E}|^2$) for different sample geometries. All near-field plots are two grating periods (1200 nm) across. Vertical dimensions are indicated beside the plots. Every near-field plot has its own gray scale. (a),(b) conformal interfaces. (c),(d) Only silver-air interface modulated. (e),(f) Only silver-quartz interface modulated. (g),(h) Both interfaces grating modulated and phase shifted against each other.

the specularly reflected beam, because the latter are on the other side of the metal film. This is an interesting aspect for surface plasmons on structured surfaces because they will not only show the exponential decay of the electromagnetic fields in the direction away from the surface, but also a field profile corresponding to the surface structure. In addition to reflection and transmission spectra, our calculations permit evaluation of the near field, which provides deep insight into the microscopic coupling behavior. Thus they allow us to optimize grating couplers in the Kretschmann-Raether arrangement with respect to the field enhancement at a particular interface, the transmission strength, or photonic band gaps in the surface plasmon dispersion.

II. REFLECTION SPECTRA

A. Theory

To calculate the reflection spectra of the layered structure with two conformally modulated interfaces sketched in the inset of Fig. 2(a), we use the Chandezon method,[12,13] which is valid even for highly modulated gratings. This formalism first maps the modulated surfaces onto parallel planes by a coordinate transformation. Then the fields are expressed in Fourier expansions in each medium and matched at the interfaces. To calculate the reflection spectra of the gratings sketched in Figs. 2(c)–2(h) with two different surfaces, we use the Chandezon technique for matching the fields at each interface. In this way we obtain two different representations for the fields inside the metal which we convert into each other by applying a point matching method[14] along a line in the middle of the metal film. The Chandezon technique also allows evaluation of the near field.[15]

All spectra in Fig. 2 are calculated for normal incidence ($\theta = 0^{\circ}$) of *p*-polarized light from the quartz side. In this polarization the electric-field vector $\vec{E}$ is perpendicular to the grating wires. The dielectric constants are taken to be $\epsilon_{\text{air}} = 1$, $\epsilon_{\text{quartz}} = 2$, and $\epsilon_{\text{silver}}(\omega)$ is an empirically determined fit function valid in the visible range.[16] For the 600 nm grating in Fig. 2(a), one finds the reflection dip representing the surface plasmon at the metal-quartz interface at 1.41 eV. If the surface plasmon at the metal-air interface could also be excited via the grating coupler, the corresponding reflection minimum should occur at about 2 eV. However, there is only the small ''diffraction edge'' caused by a vanishing diffraction order at 1.99 eV. In Fig. 2(b) we plot the field distribution of the electric field ($|\vec{E}|^2$) in all three media for $\hbar\omega$

$=1.97$ eV, an energy shortly beneath the diffraction edge. The amplitude of the incoming wave has been normalized to $|\vec{E}|_{\text{inc}}=1$. In quartz there is an interference pattern mainly formed by the incident wave, the specularly reflected beam, and the first diffraction orders. Higher diffraction orders are less important. In the air there is a standing wave and an exponential decay of the field intensity away from the silver surface. This pattern, however, is made up by the two first diffraction orders for air which are not yet propagating but still evanescent surface waves at $\hbar\omega=1.97$ eV. They interfere to give a pronounced standing wave pattern with relatively high field maxima, because they are in resonance with the grating period. The maximum field values at the silver-air interface are lower for other values of $\hbar\omega$. Even for $\hbar\omega=1.97$ eV the intensity is at least an order of magnitude lower than the field enhancement a surface plasmon would produce. Inside the metal layer the electric field shows slight concentrations in the grating valleys and at the corners, but mainly it is highest at the silver-quartz interface and decays rapidly into the silver as it would in the case of a planar metal film. As the silver layer has constant thickness, the grating coupler cannot come into effect inside the metal. For a metal film of constant thickness with two conformally modulated surfaces, on the surface opposite the incoming light, there is only the plasmon excited in attenuated total reflection at an angle greater than the total reflection angle, but there is no excitation of surface plasmons via the grating coupler at smaller angles.

In Fig. 2(c) we plot the reflection spectrum for the layer structure in which only the silver-air interface is modulated. Here, we obtain the grating coupled plasmon at the silver-quartz surface at 1.40 eV as well as the grating coupled plasmon at the silver-air interface at 1.97 eV. The near field in air for $\hbar\omega=1.97$ eV now shows a standing wave pattern formed by the plasmons propagating in the two opposite directions along the silver-air surface.The highest field intensity at the silver-air interface in Fig. 2(d) is 18 instead of 0.4 in Fig. 2(b), indicating the strong field enhancement that is characteristic of surface plasmons. In quartz, there is again an interference pattern formed by the incoming and the directly reflected wave as well as diffraction orders. The field distribution inside the silver shows that now there is strong coupling between the two surfaces across the thinnest parts of the metal layer.

For obtaining grating coupled surface plasmons at the silver-air interface, it need not necessarily be that interface that is modulated. A thickness variation of the metal layer can also be achieved by modulating the silver-quartz interface. Figure 2(e) shows the calculated reflection spectrum for this case, and as in Fig. 2(c) there is a minimum at 1.97 eV corresponding to the surface plasmon at the silver-air interface. Note that the plasmon at the silver-quartz interface at 1.40 eV also appears in the spectrum in Fig. 2(c), although the silver-quartz interface was flat in that configuration. The field distribution in Fig. 2(f) resembles very closely the one in Fig. 2(d). The coupling across the metal layer again takes place across the thin parts of the silver film, and the field enhancement at the silver-air interface is even higher.

With a metal layer that has two modulated surfaces there can be a thickness variation of the metal, if the interfaces are not conformal, for example, if the gratings are shifted against each other by a phase. We consider this case, because samples of this type can be fabricated by evaporating silver at an oblique angle onto a dielectric grating. From Fig. 2(g) we see that the plasmon at the silver-air interface at 1.98 eV is not as strong as the plasmon at the silver-quartz interface at 1.40 eV. However, they are both excited via the grating coupler. The near field for $\hbar\omega=1.98$ eV and normal incidence is plotted in Fig. 2(h). In quartz there is the usual interference pattern of the incident and the reflected waves. The electric field penetrates the silver layer most strongly where the metal layer is thinnest. Because of the phase shift between the two surfaces the thinnest part no longer is at the grating valley, but at one corner or edge instead. Correspondingly, the interference maxima of the plasmons traveling in opposite directions on the silver-air surface now get shifted from the edges [Fig. 2(d)] to the flat parts of the grating. The fact that the field maxima in air are shifted against those in the metal presents no contradiction to the continuity equations of electrodynamics. Taken separately, the $\vec{E}$-field component parallel to a surface and the component of $\epsilon\vec{E}$ perpendicular to it are continuous across each interface. As for exciting the silver-air plasmon on a planar metal film in attenuated total reflection, there is an optimal metal thickness where the plasmon excitation is strongest. Little changes in the thickness of the metal layer only change the depth and width of the reflection minimum as well as the field intensities. The metal thickness has very little influence on the field patterns. They depend on the shape of the grating. Calculated field distributions and spectra for angles of incidence other than $\theta=0^{\circ}$ will be shown in Sec. III. Each minimum splits into two for $\theta>0^{\circ}$ following the different branches of the dispersion for surface plasmons on gratings [Fig. 1(c)].

B. Measurements

We fabricated samples of the type considered in Figs. 2(g) and 2(h) and measured their reflection spectra. First, by holographic lithography a photoresist grating was prepared on top of a quartz glass substrate. The grating pattern was

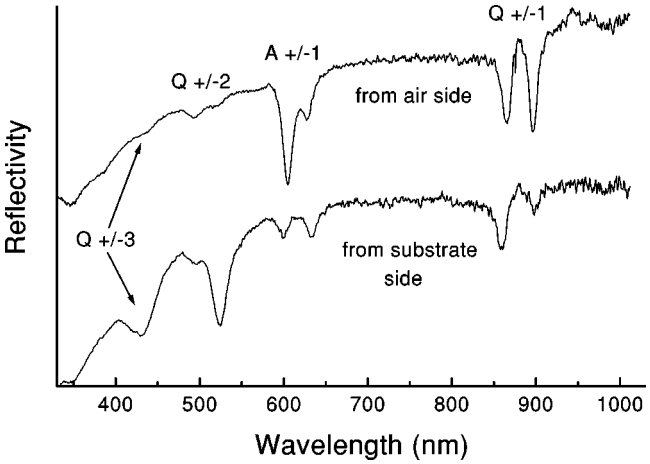

FIG. 3. Measured reflection spectra for light incidence at $\theta=1^{\circ}$ from the substrate and from the air side for a 600 nm grating with thickness modulation of the metal layer. The orders of the surface plasmon excitations on the quartz (Q) and on the air (A) side are indicated.

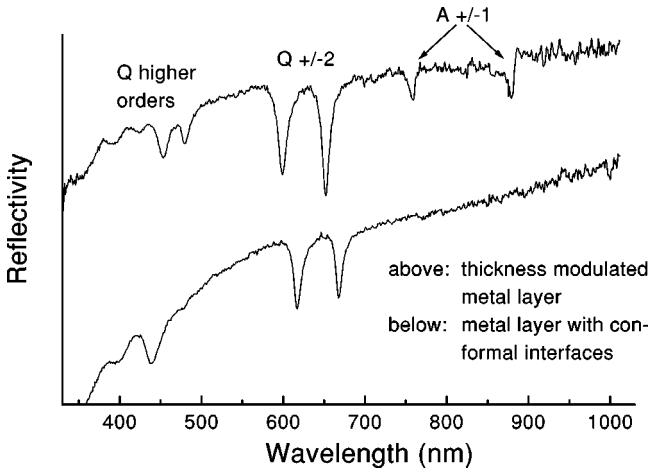

FIG. 4. Measured reflection spectra for light incidence at $\theta = 3^{o}$ from the substrate side for 800-nm gratings with and without thickness modulation of the metal layer. The orders of the plasmons are indicated as in Fig. 3.

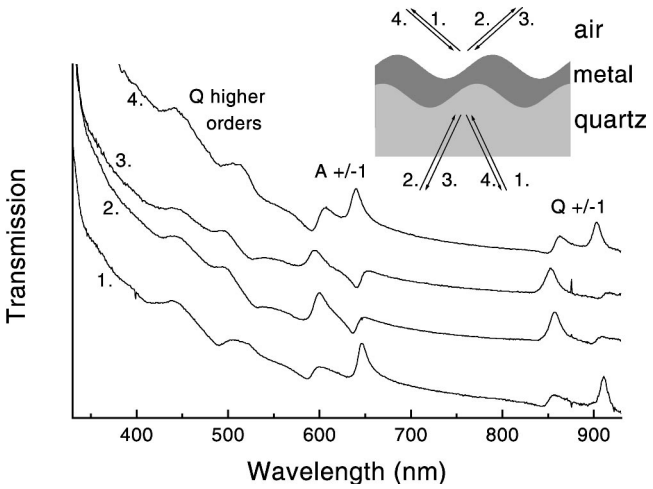

FIG. 6. Transmission spectra for a 600-nm grating with thickness modulated silver film for angles of incidence $\theta = 1.9^{o}$ from the quartz side and correspondingly $\theta = 2.7^{o}$ from air.

etched into the quartz glass by reactive ion beam etching and the photoresist was removed. Then silver was evaporated onto the grating partly at an oblique angle exploring the shadowing effect of the grating wires and partly at normal incidence to produce nevertheless a continuous metal layer. The average thickness of the silver films was about 50 nm and the modulation amplitude was 30–35 nm for both surfaces of the metal. Reflection and transmission spectra were taken with a two axis spectroscopy setup. For geometrical reasons we cannot get reflection spectra at exactly normal incidence. In Fig. 3 we show reflection spectra obtained from a sample of grating period 600 nm for light incidence at small angles from the substrate as well as from the air side. The first order grating coupled surface plasmons at the silver-air interface $A+/-1$ at about 600 nm not only appear in the upper spectrum, where the grating has been illuminated from the air side; they are also present in the lower spectrum, where light incidence was from the quartz side. Equivalently, the first order grating coupled plasmons at the silver-quartz interface $Q+/-1$ around 880 nm are seen in both spectra. The higher order surface plasmons at the silver-quartz interface $Q+/-2$ and $Q+/-3$ at wavelengths below 550 nm, clearly pronounced when shining in the light from the quartz side, get considerably weaker for illumination from the air side. They can still be distinguished in the upper spectrum as well though.

Figure 4 shows a spectrum obtained from an 800 nm grating at an angle of incidence $\theta = 3^{o}$ with illumination from the quartz side. The first order grating coupled silver-air surface plasmons $A+/-1$ are clearly observed at 756 nm and 878 nm. For this grating period the first order silver-quartz plasmons are at wavelengths beyond the range of our light source and detector, but the second order modes $Q+/-2$ are found around 630 nm and higher order ones between 400 and 500 nm. For comparison, we also measured the reflection of an 800 nm grating onto which the silver has been

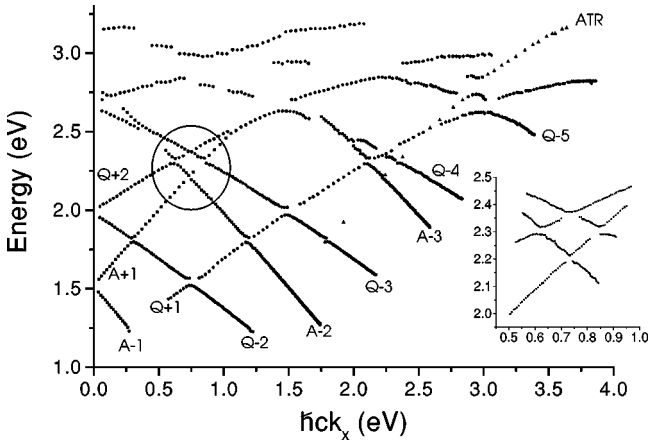

FIG. 5. Minimum positions from reflection spectra for an 800-nm grating with thickness modulated metal layer for light incidence from the quartz side. Circles: silver-quartz plasmons. Squares: silver-air plasmons. Triangles: silver-air plasmon excited in attenuated total reflection beyond the total reflection angle. The inset shows a measurement in finer angular steps of the region marked by the big circle.

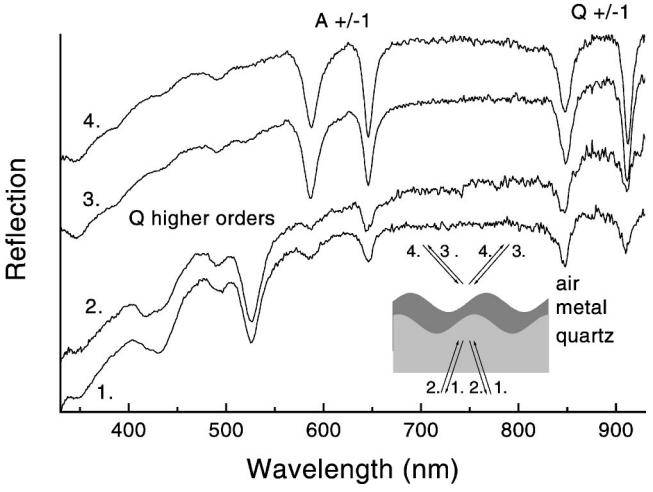

FIG. 7. Reflection spectra for a 600-nm grating for angles of incidence $\theta = 2^{o}$ from quartz and $\theta = 3^{o}$ from air.

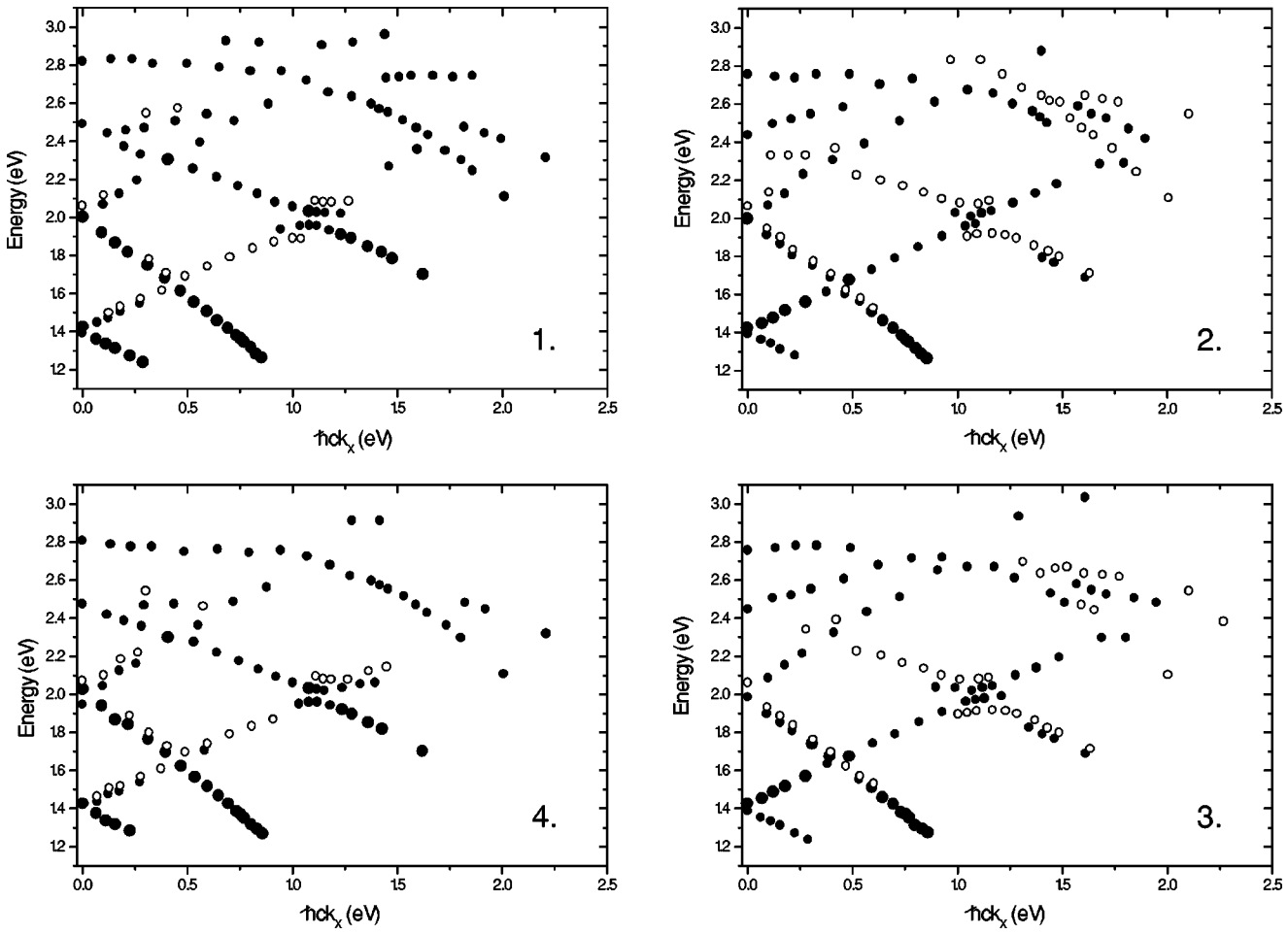

FIG. 8. Positions in wave vector and energy of the minima and maxima from transmission spectra of a 600-nm grating in all four possible geometries. Numbers 1–4 designate the same configurations as in Fig. 6. Large full circles: ''great maxima.'' Small full circles: normal maxima. Small open circles: minima.

evaporated perpendicularly only. We verify that silver-air plasmons $A+/-1$ do not appear for illumination of the grating from the quartz side. Ion beam etching produces sharp edges which the evaporation process will smooth out a little. However, the absence of the silver-air plasmons in the reflection spectrum confirms that the two interfaces are nearly conformal and there is no significant thickness variation of the metal layer in this sample. The positions of the second order silver-quartz plasmons $Q+/-2$ are shifted a little against those of the sample with thickness modulation and some of the higher order modes vanish towards small angles of incidence. These effects should be due to the different sample geometries, but we do not have detailed explanations for these peculiarities yet.

For the 800 nm grating with the thickness modulated silver film the positions in energy and wave vector of the reflection minima are displayed for all angles of incidence in the diagram in Fig. 5. The dispersion branches of the silver-quartz and the silver-air plasmons can clearly be distinguished by their slope. The steeper ones belong to the surface plasmons on the air side. An interesting region around $\hbar ck_x \approx 0.75$ eV and $\hbar\omega \approx 2.25$ eV, where dispersion branches of surface plasmons from both interfaces meet, has been measured in finer angular steps and is shown in greater detail in the inset. There is anticrossing, indicating interaction between surface plasmon modes on the same side of the metal as well as between surface plasmons on different sides of the thin metal film. Photonic band gaps open up in the dispersion of surface plasmons propagating in the direction perpendicular to the grating wires. The minimum positions in Fig. 5 are gathered from reflection spectra for illumination from the quartz side. The silver-air plasmon excited in attenuated total reflection shortly beyond the total reflection angle, as for a planar metal film, is observed up to very high energies. Apart from that, at energies above roughly 2.7 eV only the surface plasmons on the quartz side are discernible. For illumination from the air side the silver-air plasmons can be tracked down to higher energies than the silver-quartz plasmons. In each case the surface plasmons on the second interface are weaker than the plasmons on the interface directly illuminated by the incident light. The latter dominate at higher energies where the dispersion branches are much closer to each other. Up to that region, however, we clearly observe surface plasmons on both sides of the thickness modulated silver films, no matter from which medium the grating is illuminated. All spectra come out absolutely flat for *s* polarization. As surface plasmons can only be excited in *p* polarization, this proves that the minima in our reflection spectra cannot be caused by diffraction effects, but are indeed due to surface plasmons.

III. TRANSMISSION SPECTRA

A. Experiments

Transmission spectra for the 600 nm grating with illumination from the substrate and from the air side are shown in Fig. 6. The shadowing effect during the metal evaporation, which is needed to yield the thickness modulation, produces an asymmetric grating profile. Thus the two directions towards which the angle of incidence can be tilted from the grating normal are not equivalent. The two transmission spectra obtained with the light incident from the substrate side as well as the two spectra for which the beam was incident from the air side are quite different from one another. Nevertheless, the four curves plotted in Fig. 6 consist of two pairs of very similar spectra. In each case these are the ones for which the light path has been reversed. The corresponding reflection spectra have been plotted for comparison in Fig. 7. The reflection spectra vary according to whether they have been taken from the glass or from the air side. However, there is no significant difference for the two directions the incident beam can have with respect to the asymmetric grating profile. That is, for the two identical reflection spectra taken from the substrate side as well as for the two taken from the air side, the corresponding transmission spectra are not identical. Or, put the other way round, for the one as well as for the other beam direction with respect to the grating profile, the zeroth order transmission spectra are almost identical, no matter if the light is transmitted from the substrate to the air side or vice versa,[9,10] but the corresponding reflection spectra are different for the two sides of the metal.

In the reflection spectra surface plasmons are seen as minima. In transmission they can appear as maxima (e.g., Fig. 6, spectrum 2, 600 nm), as minima (e.g., Fig. 6, spectrum 2, 635 nm) or have a Fano-type resonance shape (e.g., Fig. 6, spectrum 1, 590 nm). Certain maxima are strikingly high and sharp. They shall be designated as ''great maxima'' (e.g., Fig. 6, spectrum 1, 645 nm), although the boundary to ''normal'' maxima is somewhat arbitrary. Apart from the continuous rise towards lower wavelengths, all transmission spectra come out absolutely flat in *s* polarization. So we know that, as for the reflection spectra, all features in our transmission spectra are caused by surface plasmons. The positions of maxima and minima from the transmission spectra for the four possible geometries for the 600 nm grating are shown in Fig. 8. A Fano-shaped resonance in a spectrum has been marked as a maximum and a minimum closely together. The numbers 1–4 stand for the same configurations as in Fig. 6. Diagrams 1 and 4 as well as 2 and 3, which by pairs belong to the same geometry with only the light path reversed, are very similar to one another as explained above for the spectra in Fig. 6. One also notices that these two pairs of diagrams are complementary. At least for the lower order modes, which can be clearly disentangled in the spectra, minima in the two left plots correspond to maxima in the two right plots and vice versa. ''Great maxima'' in the plots on the left correspond to weaker ones or Fano-type resonances in the plots on the right and vice versa. Another characteristic feature is that in one diagram minima constitute rising or falling branches but never rising and falling branches in one and the same of the four plots. That is, if minima belong to positive (negative) grating orders, they do so for the silver-air and the silver-quartz plasmons. The same does not hold true entirely for the ''great maxima.'' In plots 2 and 3 the falling branch of the silver-air plasmon starting at 2 eV is seen as a rather strong maximum at lower energies compared to the other structures in the spectra at larger angles of incidence. However, the branch is a Fano-type resonance until beyond the crossing with the first order quartz plasmon. Thus the general trend is that for the light paths 1 and 4 the falling branches of the surface plasmon dispersion result in pronounced maxima in transmission, whereas the rising branches can even manifest themselves as minima in the spectra. For the light paths 2 and 3 the falling branches are minima or at least weaker maxima than the rising ones. This complementary behavior of the rising and falling dispersion branches is found for our other samples with thickness modulated silver layer of different grating periods, too.

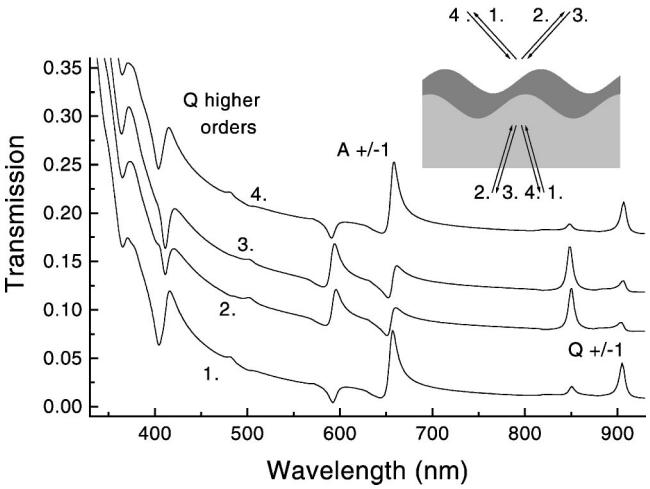

FIG. 9. Calculated zeroth-order transmission spectra for a 600-nm grating with thickness modulated silver film for angles of incidence $\theta = 2^{o}$ from quartz and $\theta = 3^{o}$ from air. Numbers refer to the same configurations as in Fig. 6. The upper three spectra have been shifted upwards for clearness.

B. Calculations

In analogy to Figs. 6 and 7, Figs. 9 and 10 show calculated transmission and reflection spectra for small angles of incidence. The numbers refer to the same configurations as in Figs. 6 and 7. The grating period is 600 nm. The distance between the highest points of the two interfaces of the metal has been set to 50 nm. The modulation amplitude is 35 nm for the silver-air interface and 30 nm for the silver-quartz interface. The grating profiles of the two interfaces have slightly different pitch and they are shifted against each other by a phase of 77^{o} (360^{o} corresponds to a whole grating period) to achieve the thickness modulation of the metal. The results are in qualitative agreement with the experiment. In transmission the correct surface plasmon modes come out as maxima, minima, or Fano-type resonances, respectively. Only the slight differences between minima and Fano-shaped resonances are not reproduced very well by the calculations. In the calculated reflection spectra the silver-air plasmons are much weaker than the silver-quartz plasmons for illumination from the quartz side, and the silver-quartz plasmons are much weaker than the silver-air plasmons for illumination

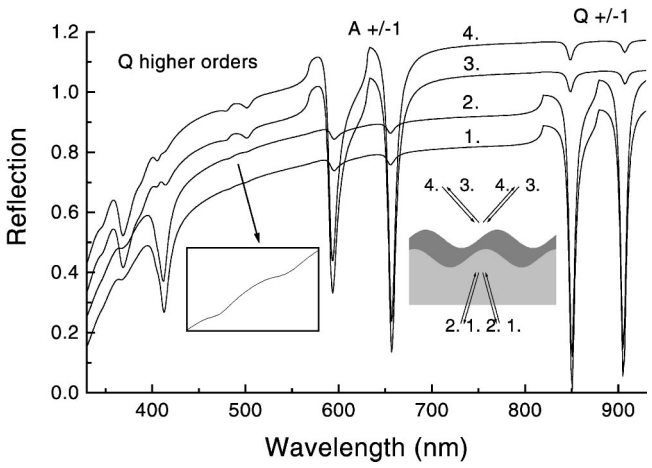

FIG. 10. Calculated zeroth-order reflection spectra for the same parameters as the transmission spectra in Fig. 9. Numbers refer to the same cases as in Fig. 7. The upper curves have been successively shifted in the vertical direction.

from the air side. In our aim to get grating coupled surface plasmons on the interface not facing the incoming light the experimental results are even better than our calculations predict. The absorption minima from the plasmons on the two sides of the metal are much less differently deep in the measured reflection spectra. Strangely, for the chosen parameters the second order quartz modes around 500 nm are almost absent in the calculated reflection spectra, particularly for illumination from the quartz side (Fig. 10).

The calculated transmission and reflection spectra for the four possibilities of the light path come in pairs just like the experimental curves. The two spectra for reflection at the substrate side of the grating are identical as well as the two reflection spectra at the air side. The transmission spectra depend on the direction the light beam has with respect to the asymmetric grating profile, but they are identical for reversed light paths.

To understand the difference between a mode that appears as a maximum in the transmission spectra and one that appears as a minimum, in Fig. 11 we plot the field distributions for the minima at 649 nm and the maxima at 596 nm in spectra 2 and 3 of Fig. 9. As in the corresponding reflection spectrum the silver-air plasmons are only small absorption minima for illumination from the quartz side, the field enhancement at the air side in Figs. 11(a) and 11(b) is not as strong as in Figs. 2(d), 2(f), and 2(h). The field intensity is clearly higher though than in Fig. 2(b) where there is no surface plasmon. The characteristic feature is that, when the silver-air plasmons are excited with the light incident from the quartz side, for the mode at 649 nm that occurs as a minimum or Fano-type resonance in the zeroth order transmission spectrum there is a field enhancement reaching across the metal in the part protruding into the air [Fig. 11(a)]; a less coarse gray scale would reveal a bottlenecklike connection between the bulges on both sides. For the mode at 596 nm that is seen as a maximum in the transmission spectrum [Fig. 11(b)] the coupling across the metal takes place not only across the thinnest part, but also across the flat part protruding towards the quartz. This correlation between the field distribution and the appearance of a mode in transmission is generally fulfilled for incidence angles other than $\theta=0^{o}$. Sometimes the modes of the same positive and negative order are both maxima in transmission, but then one is considerably weaker than the other. In this case this mode of much less efficient transmission takes the role of the minimum. For $\theta=0^{o}$ the strongest fields in the metal are found where the metal is thinnest (see Fig. 2), which is at one of the grating edges for our sample geometry. For other angles of

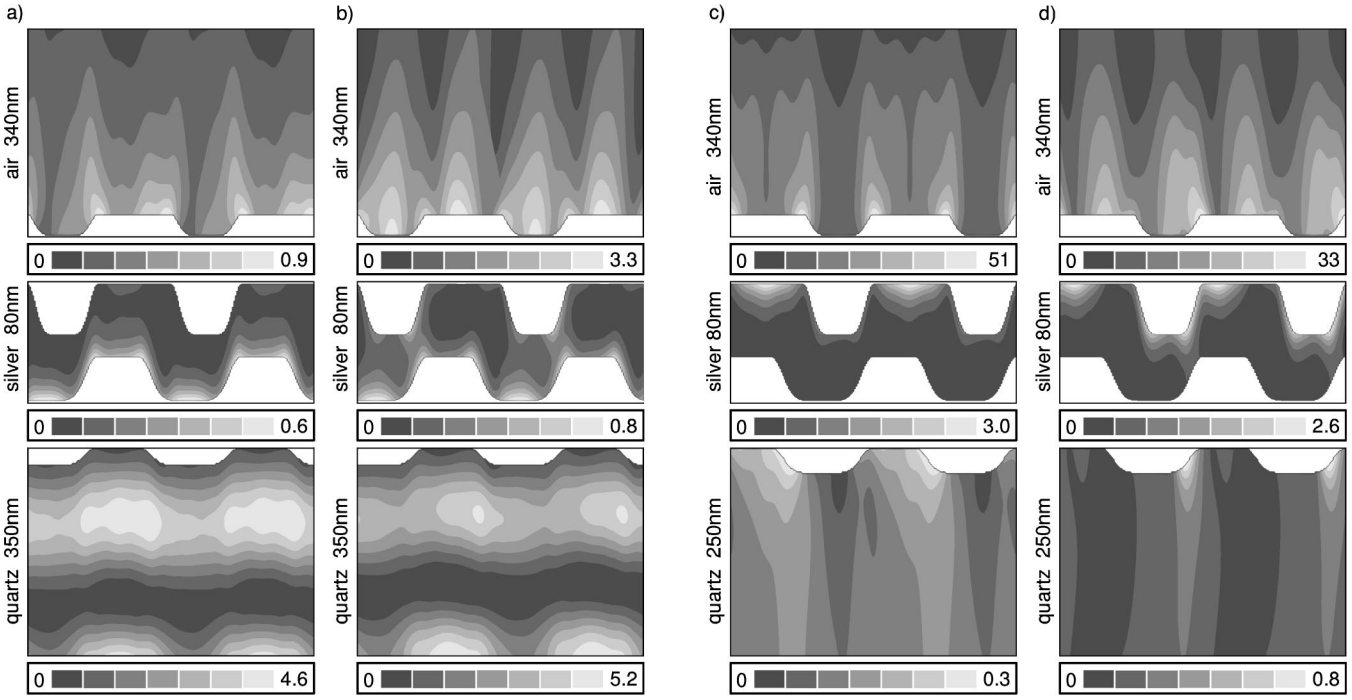

FIG. 11. Field distributions corresponding to (a) the minimum at 649 nm in spectrum 2 of Fig. 9. (b) The maximum at 596 nm in spectrum 2 of Fig. 9. (c) The minimum at 649 nm in spectrum 3 of Fig. 9. (d) The maximum at 596 nm in spectrum 3 of Fig. 9.

incidence the field maximum is shifted to either the flat part of the grating or additional regions of high electric field start to occur there.

When the light is incident from the air side, the silver-air plasmons are excited like they would be on a single modulated interface. The field enhancement at this interface is much stronger in this case, of course. The near-field distributions in Figs. 11(c) and 11(d) are different from the ones in Figs. 11(a) and 11(b). Therefore, it is astonishing that the respective transmission spectra are identical (Fig. 9). If the plasmon excitation is on the first interface directly illuminated by the incoming light, a correlation between the field distribution and the appearance of the plasmon mode as a minimum or a maximum in the transmission spectrum is much less evident. The preference for the enhanced fields in the metal to occur at the flat part protruding into the air in Fig. 11(c) and at the thinnest part in Fig. 11(d) bears some faint resemblance to Figs. 11(a) and 11(b), however. This suggests that for plasmons on the first interface the rule formulated in the preceding paragraph for plasmons on the second interface has to be reversed: A high electric field in the part of the metal layer nearer to the incoming light for a transmission minimum and in the part farther away from the incoming light for a transmission maximum. From the field distributions in quartz one can imagine that there is better transmission for the plasmon mode at 596 nm [Fig. 11(d)] than for the one at 649 nm [Fig. 11(c)], because in Fig. 11(d) there is a field enhancement creeping up the edge[11,17] in the direction of the transmitted beam (see light path 3 in Fig. 9).

IV. CONCLUSIONS

We have performed calculations and experiments on grating coupler induced surface plasmons in the Kretschmann-Raether configuration. We find that for excitation of surface plasmons on that surface of a thin modulated metal film that is not directly facing the incident light a thickness modulation of the metal layer is required. A metal film of uniform thickness, however modulated, is not sufficient for this purpose. In principle, there are different ways of achieving a thickness variation of the metal layer. One can modulate any one of the two surfaces or modulate both and shift the gratings against each other. Samples of the last kind have been prepared and investigated spectroscopically in reflection and transmission. In the reflection spectra the surface plasmons are seen as minima. In transmission some modes occur as minima or Fano-shaped resonances, while others appear as maxima. This behavior is correlated to the field distribution inside the metal layer.

ACKNOWLEDGMENT

We thank the Deutsche Forschungsgemeinschaft (DFG) for financial support under Grant No. DFG He1938/2-2.

[1] H. Raether, *Surface Plasmons*, edited by G. Höhler, Springer Tracts in Modern Physics Vol. 111 (Springer, Berlin, 1988).
[2] H. Yokota, K. Saito, and T. Yanagida, Phys. Rev. Lett. **80**, 4606 (1998).
[3] J. Koglin, U. C. Fischer, and H. Fuchs, Phys. Rev. B **55**, 7977 (1997).
[4] L. Novotny, D. W. Pohl, and B. Hecht, Ultramicroscopy **61**, 1 (1995).
[5] M. Specht, J. D. Pedarnig, W. M. Heckl, and T. W. Hänsch, Phys. Rev. Lett. **68**, 476 (1992).
[6] W. L. Barnes, S. C. Kitson, T. W. Preist, and J. R. Sambles, J. Opt. Soc. Am. A **14**, 1654 (1997).
[7] S. C. Kitson, W. L. Barnes, and J. R. Sambles, Phys. Rev. Lett. **77**, 2670 (1996).
[8] S. C. Kitson, W. L. Barnes, and J. R. Sambles, J. Appl. Phys. **84**, 2399 (1998).
[9] T. W. Ebbesen, H. J. Lezec, H. F. Ghaemi, T. Thio, and P. A. Wolff, Nature (London) **391**, 667 (1998).
[10] H. F. Ghaemi, T. Thio, D. E. Grupp, T. W. Ebbesen, and H. J. Lezec, Phys. Rev. B **58**, 6779 (1998).
[11] U. Schröter and D. Heitmann, Phys. Rev. B **58**, 15 419 (1998).
[12] J. Chandezon, M. T. Dupuis, G. Cornet, and D. Maystre, J. Opt. Soc. Am. **72**, 839 (1982).
[13] W. L. Barnes, T. W. Preist, S. C. Kitson, and J. R. Sambles, Phys. Rev. B **54**, 6227 (1996).
[14] R. Petit, in *Electromagnetic Theory of Gratings*, edited by R. Petit, Topics in Current Physics Vol. 22 (Springer, Berlin, 1980).
[15] W. L. Barnes, T. W. Preist, S. C. Kitson, J. R. Sambles, N. P. K. Cotter, and D. J. Nash, Phys. Rev. B **51**, 11 164 (1995).
[16] $\epsilon(\lambda) = -219.945 - 0.026\,169\,5\lambda + 3.8559\sqrt{\lambda} + 4857.2/\sqrt{\lambda} + i(7.139 + 0.001\,656\lambda - 0.2129\sqrt{\lambda})$, λ in Å.
[17] U. Schröter, S. Seider, S. Tode, and D. Heitmann, Ultramicroscopy **68**, 223 (1997).